

Reaction Mechanisms and Kinetics of Xylo-Oligosaccharide Hydrolysis by Dicarboxylic Acids

Youngmi Kim, Thomas Kreke, and Michael R. Ladisch

Laboratory of Renewable Resources Engineering, Purdue University, West Lafayette, IN 47907

Dept. of Agricultural and Biological Engineering, Purdue University, West Lafayette, IN 47907

DOI 10.1002/aic.13807

Published online April 23, 2012 in Wiley Online Library (wileyonlinelibrary.com).

Hydrothermal pretreatment of lignocellulosic materials generates a liquid stream rich in pentose sugar oligomers. Cost-effective hydrolysis and utilization of these soluble sugar oligomers is an integral process of biofuel production. We report integrated rate equations for hydrolysis of xylo-oligomers derived from pretreated hardwood by dicarboxylic maleic and oxalic acids. The highest xylose yield observed with dicarboxylic acids was 96%, and compared to sulfuric acid, was 5–15% higher with less xylose degradation. Dicarboxylic acids showed an inverse correlation between xylose degradation rates and acid loadings unlike sulfuric acid for which less acid results in less xylose degradation to aldehydes and humic substances. A combination of high acid and low-temperature leads to xylose yield improvement. Hydrolysis time course data at three different acid concentrations and three temperatures between 140 and 180°C were used to develop a reaction model for the hydrolysis of xylo-oligosaccharides to xylose by dicarboxylic acids. © 2012 American Institute of Chemical Engineers AIChE J, 59: 188–199, 2013

Keywords: xylo-oligomers, hemicellulose hydrolysis, acid catalyst kinetics, maleic acid, oxalic acid

Introduction

Hemicellulose, which represents 15–35% of lignocellulosic biomass, is made of complex, heterogeneous polysaccharides, consisting primarily of xylan and smaller amounts of arabinan, galactan, uronic, and acetic acid.^{1–3} Hydrothermal pretreatments, such as steam explosion and liquid hot water, efficiently fractionate hemicellulose away from lignocellulosic materials by dissolution.^{4–6} Hydronium ions generated from autoionization of water at an elevated temperature cause acetic acid to be released from the hemicellulose as well as catalyze formation of oligomers by partial hydrolysis of hemicellulose.⁴ Posthydrolysis of these oligomers results in monosaccharides that may be converted to biofuels and other chemicals.^{2,3,7,8} A broad array of hemicellulolytic enzymes is required to fully depolymerize the oligosaccharides through hydrolysis of xylan backbone and removal of acetyl, arabinan, and uronic acid side substituents.^{1–3} Acid catalysis offers two main advantages over enzymatic hydrolysis: short reaction time and reduced catalyst cost.^{7,8}

Dicarboxylic, organic acids (maleic acid, oxalic acid, and fumaric acid) have been identified as suitable hydrolytic molecules. They are less corrosive, more selective, and may be thermally decomposed into nontoxic molecules (CO₂, formic, and fumaric acids) at the end of their use cycle, unlike sulfuric acid.^{9–14} Maleic acid, which mimics the structure of the active site in cellulase enzymes, has selectivity superior to sulfuric acid hydrolysis of sugar polymers due to lower sugar degradation.^{9–12} Oxalic acid, another dicarboxylic acid,

is secreted by brown-rot fungi that degrade fiber structures in plant materials¹⁵ and has demonstrated potential for hydrolysis of lignocellulosic materials.^{16–20}

The higher selectivity of the organic dicarboxylic acids, compared to sulfuric and hydrochloric acids, is consistent with their structure that resembles the catalytic core of cellulase.^{11,12} Cellulase enzymes, like diacids, harbor two carboxylic residues, which catalyze the hydrolysis of cellulose.¹⁰ These carboxylic groups, one serving as a proton donor while the other serving as a nucleophile, are 4–10 Å apart and catalyze the hydrolysis through general acid catalysis.²¹ Similarly, the strong internal hydrogen bonding (2.5 Å) between the two carboxylate ends of maleic acid results in effective general acid catalysis, mimicking cellulase catalyzed hydrolysis.²²

Despite their promising catalytic features, there are only a handful of studies that have investigated the organic dicarboxylic acid-catalyzed hydrolysis of plant-derived polysaccharides. Moreover, most of the previous studies involving these weak acids examined a limited range of conditions, and the results were often compared to sulfuric acid based on separate studies that were applied to different feedstocks, reaction conditions, and equipment.

This work reports a mathematical kinetic model for acid-catalyzed hydrolysis of soluble xylo-oligomers by dicarboxylic acids (maleic and oxalic acids) and compares these results to sulfuric acid. The xylo-oligosaccharide solution was obtained from a common feedstock, that is, the liquid from aqueous pretreatment of mixed hardwood. A classic homogeneous, pseudo-first-order hydrolysis kinetics was found to accurately represent the hydrolysis of xylo-oligomers by all three acids, with differences between sulfuric, oxalic, and

Correspondence concerning this article should be addressed to M. R. Ladisch at ladisch@purdue.edu.

maleic acids being captured through the kinetic parameters. This model enabled us to identify, assess, and compare catalytic performance and to determine optimal hydrolysis conditions, together with a mechanistic explanation of how the selected model represents the hydrolysis mechanism.

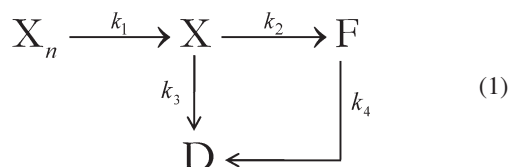
Reaction Model

Acid hydrolysis of hemicellulose in lignocellulosic materials is often modeled as a monophasic consecutive pseudo-first-order reaction that follows the general cellulose hydrolysis kinetics model proposed by Saeman.²³ Later, a biphasic model was introduced by Kobayashi and Sakai²⁴ in which hemicellulose in lignocellulose was categorized into two types based on the reactivity to acid hydrolysis: fast-hydrolyzing hemicellulose and slow-hydrolyzing hemicellulose. This was based on the observation that, in a typical xylan hydrolysis, the hydrolysis rate decreased after about 65–70% of the initial available xylan was hydrolyzed and was found to be consistent with observed hydrolysis of hemicellulose in corn stover.^{3,10,25} Other studies have reported that the susceptible fraction of xylan in biomass is 0.7–0.89.^{26–28}

In this study, we used a monophasic model based on Saeman's pseudohomogeneous irreversible first-order reaction kinetics as both the hardwood-derived xylo-oligomers and dicarboxylic and sulfuric acids are soluble in water. As the reaction occurs in a homogeneous liquid phase, mass-transfer limitation due to pore diffusion can also be neglected. We assumed that the soluble xylo-oligomers represent the fast-hydrolyzing hemicellulose of Kobayashi and Sakai.²⁴ Hydrothermal pretreatment solubilizes 70–80% of initial xylan present in hardwood and would correlate to the amount of easy-to-hydrolyze hemicellulose in hardwood.³

Degradation of xylose by acids generates furan aldehydes, mainly furfural, which further degrades to humic substances. A simplified model was given by Root²⁹ and Harris et al.³⁰ and later adopted in other studies.^{31,32} In this model, intermediates formed during the course of xylose dehydration to furfural are also directly decomposed to degradation products. The humins and other degradation products are formed by a reaction between xylose or xylose intermediates and furfural. Hence, xylose dehydration to furfural and humic substances was also generally modeled as a consecutive first-order reaction.^{2,10,32}

The simplified, overall kinetic model used in this study is as follows^{23,29,30}:



where X_n = xylo-oligomers; X = xylose; F = furfural; D = degradation products (humins). Based on the model above, the following set of differential equations was derived:

$$\frac{d[X_n]}{dt} = -k_1 \cdot [X_n] \quad (2)$$

$$\frac{d[X]}{dt} = k_1 \cdot [X_n] - k_2 \cdot [X] - k_3 \cdot [X] \quad (3)$$

$$\frac{d[F]}{dt} = k_2 \cdot [X] - k_4 \cdot [F] \quad (4)$$

Solving the above equations gives the integrated rate equations for the concentration of xylo-oligomers, xylose, and furfural:

$$[X_n] = [X_n]_{t=0} \exp^{-k_1 t} \quad (5)$$

$$[X] = \frac{k_1 [X_n]_{t=0}}{k_1 - k_2 - k_3} \left(\exp^{-(k_2+k_3)t} - \exp^{-k_1 t} \right) + [X]_{t=0} \exp^{-(k_2+k_3)t} \quad (6)$$

$$\begin{aligned}
 [F] = & \frac{k_1 k_2 [X_n]_{t=0}}{k_1 - k_2 - k_3} \left\{ \frac{1}{k_2 + k_3 - k_4} \left(\exp^{-k_4 t} - \exp^{-(k_2+k_3)t} \right) \right. \\
 & \left. - \frac{1}{k_1 - k_4} \left(\exp^{-k_4 t} - \exp^{-k_1 t} \right) \right\} \\
 & + \frac{k_2 [X]_{t=0}}{k_2 + k_3 - k_4} \left(\exp^{-k_4 t} - \exp^{-(k_2+k_3)t} \right) + [F]_{t=0} \exp^{-k_4 t} \quad (7)
 \end{aligned}$$

in which X_n , X , F , and D are the concentration of xylo-oligosaccharides, xylose, furfural, and degradation products (humic solids), respectively (g/L); t = time (h); k = rate constant (1/h).

The time at which xylose concentration reaches its maximum is given by:

$$t_{\max} = \frac{\ln \left(\frac{k_2+k_3}{k_1} \right)}{k_2 + k_3 - k_1} \quad (8)$$

Another term that can be derived from the above equations is selectivity factor, which is defined as a ratio of xylo-oligosaccharide hydrolysis rate to xylose degradation rate.¹² Higher selectivity factors represent higher xylose yields. Selectivity of xylose formation is:

$$\text{Selectivity factor} = \frac{k_1}{k_2 + k_3} \quad (9)$$

The rate constant, k is correlated to temperature and acid concentration by Arrhenius equation^{3,9,10,23}:

$$k = K \cdot \exp \frac{E}{RT} \quad (10)$$

$$K = k_0 \cdot [H^+]^m \quad (11)$$

where K is the pre-exponential factor; $[H^+]$ is the measured initial aqueous hydronium ion concentration at room-temperature (M); E is the activation energy (cal/mol); R is the ideal gas law constant [1.98 cal/(mol K)]; and T = temperature (K). The rate constants in this study should be regarded as “observed” or “apparent” rate constants that include lumped effects of proton, acid, base, ionic strength, and buffering capacity of the substrate on the hydrolysis kinetics.

In many early studies, the rate constant was correlated to acid concentration by weight percent. However, lignocellulose contains minerals and compounds that buffer or neutralize an added acid. Consequently, attempts have been made to more accurately relate the rate constants to acid catalysts by incorporating aqueous hydronium ion concentrations rather than acid concentrations in the rate constant expressions.³ Such an approach has been adapted in our study as well, recognizing that the xylo-oligosaccharide solution contains minerals and other compounds that neutralize acids. Thus, throughout this study, $[H^+]$ represents actual measured

Table 1. Composition of the Xylo-oligosaccharide Solution Obtained from Steam Pretreated Mixed Hardwood

Components	As Received	Standard Deviation	After Acid Solution Added
Gluco-oligomers (glucose equivalent)	3.5	0.4	2.9
Xylo-oligomers (xylose equivalent)	64.2	3.1	53.5
Glucose	0.4	0.1	0.3
Xylose	9.9	0.7	8.3
Lactic acid	0.5	0.4	0.4
Glycerol	0.6	0.1	0.5
Acetic acid (free)	6.1	0.1	5.1
Acetyl (bound)	13.5	0.2	11.3
Butanediol	0.1	0.1	0.1
HMF	nd	0.1	nd
Furfural	nd	0.0	nd

nd: not detected.

hydronium ion concentration using pH measured at room temperature. Acid dissociation is also known to depend on temperature.³³ The temperature effect on acid dissociation was not factored in our kinetic model, as the temperature dependence of carboxylic acid's dissociation constants is generally negligible (<10% compared to 25°C) over the range of temperatures used in this study.^{34,35} Thus, kinetic parameters were calculated based on measured rates and extents of reactions for acids starting at the same measured initial pH. This approach enabled us to simplify the model, compare the kinetic constants of different acids based on the same measurable parameter (pH), and identify the key kinetic parameters that differentiate the acids from each other.

Xylose and furfural yields were calculated by equations below.

$$\% \text{ xylose yield} = \frac{[X]_{t=t}}{[X]_{t=0} \cdot \frac{150}{132} + [X]_{t=0}} \quad (12)$$

$$\% \text{ furfural yield} = \frac{[F]_{t=t}}{([X]_{t=0} \cdot \frac{150}{132} + [X]_{t=0}) \cdot \frac{96.1}{150}} \quad (13)$$

The parameter 150/132 represents the ratio of molecular weight of xylose to anhydro-xylose to account for the gain of one water molecule per xylose molecule as the xylose-oligosaccharides are hydrolyzed to xylose. The ratio 96.1/150 represents the ratio of molecular weight of furfural to xylose.

The severity factor, which gives a numerical representation of the combined temperature and residence time and reaction severity, is defined as³⁶:

$$\log R_0 = \log \left[t \cdot \exp \left(\frac{T - 100}{14.75} \right) \right] \quad (14)$$

where t = time (h); T = temperature (°C).

Experimental Procedures

Materials

The xylo-oligomers-containing sugar solution at pH 3.7 was kindly provided by Mascoma Corporation (Lebanon, NH). The xylo-oligosaccharides were derived from mixed hardwood that mainly comprises poplar. Composition of the xylo-oligosaccharide solution was analyzed using LAP 014³⁷ (Table 1). Sulfuric ($pK_a = -3$ and 2.0), maleic ($pK_a = 1.9$

and 6.1), oxalic acids ($pK_a = 1.3$ and 4.1), and all other reagents and chemicals, unless otherwise noted, were purchased from Sigma-Aldrich (St. Louis, MO).

Acid hydrolysis of xylo-oligomers

Each batch of hydrolysis was carried out with 2.4 mL solution consisting of a mixture of 2 mL xylo-oligosaccharide and 0.4 mL acid solutions with compositions as shown in Table 1. Addition of acid stock solution diluted the sugars by 1.2 times.

Sulfuric acid was varied from 19 to 102 mM (1.9–10 mg/mL) to give pH's ranging from 1.3 to 2.2 in the final mixture. Maleic acid at 50–172 mM (5.8–20 mg/mL) gave pH 1.7–2.2 and oxalic acid at 33–132 mM (3–12 mg/mL) gave pH 1.5–2.2. Hydronium ion (pH) as a function of acid concentration is shown in Figure 1A. Approximately three times more maleic acid and 1.4 times more oxalic acid were required to give the same pH as sulfuric acid.

Hydrolysis reactions were conducted in 3/8 in. OD \times 0.03 in. wall thickness (0.95 cm \times 0.08 cm), 316 stainless steel tubing capped at either end with 3/8 in. Swagelok tube end fittings (Swagelok, Indianapolis, IN).⁵ Each tube was 3 in. (7.6 cm) in length and 4 mL in total volume. The sample

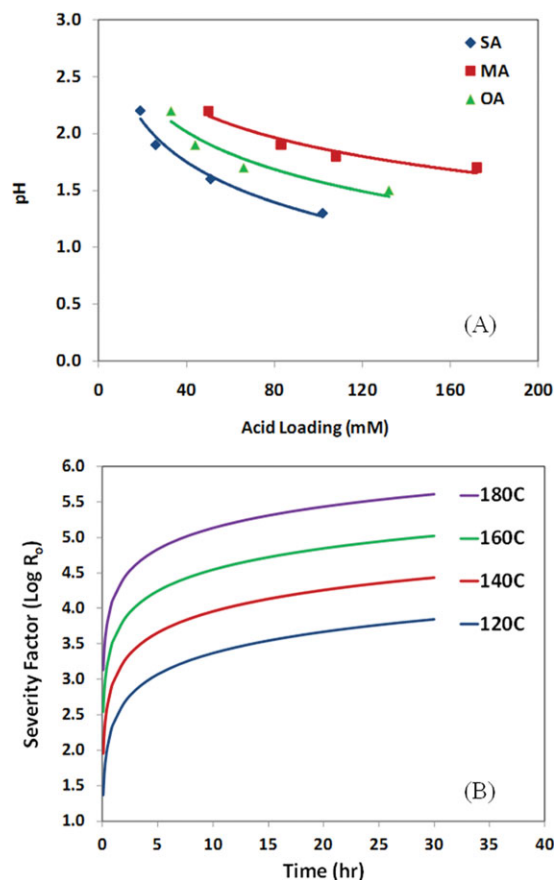


Figure 1. (A) The pH of xylo-oligosaccharide solution at different acid loadings of sulfuric, maleic, and oxalic acid.

Data represent average of duplicate measurements; (B) severity factor versus hydrolysis time at temperatures between 120 and 180°C. SA: sulfuric acid; MA: maleic acid; OA: oxalic acid. [Color figure can be viewed in the online issue, which is available at www.interscience.wiley.com.]

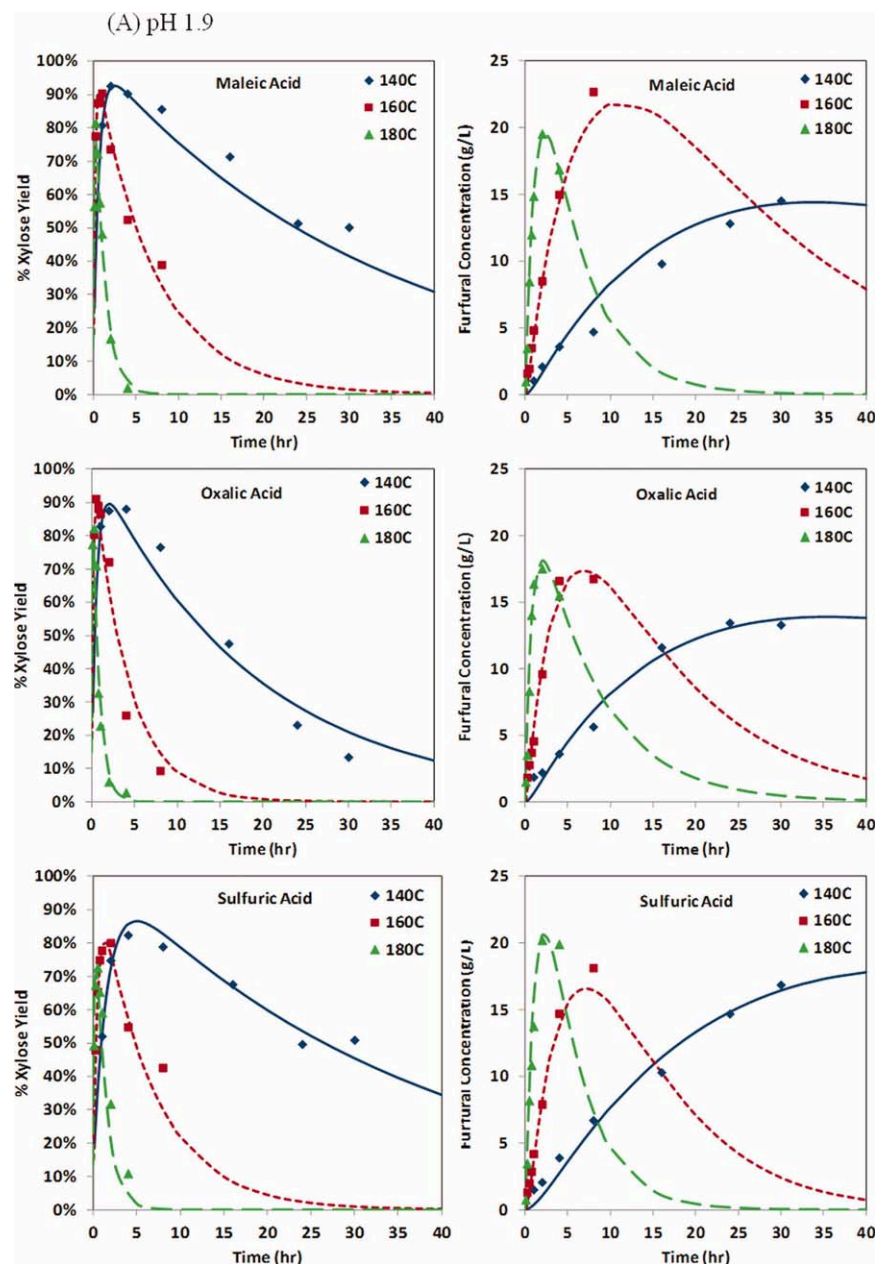


Figure 2. Experimental (symbols) and calculated (lines) xylose yields and furfural concentrations (A) at initial pH 1.9 and various temperatures and (B) at 140°C and different initial pH (acid loadings) for sulfuric, maleic, and oxalic acids.

Each data point represents an average of duplicate runs. [Color figure can be viewed in the online issue, which is available at wileyonlinelibrary.com.]

volume of 2.4 mL gave 40% head space for liquid expansion during the reaction. The sample was heated by placing the tube in a Tecam® SBL-1 fluidized sand bath (Cole-Parmer, Vernon Hills, IL) set to a target temperature. Reaction temperature and time were varied from 120 to 180°C and 1 min to 30 h, respectively. Time and temperature were varied to give a range of thermal severity factors over which hydrolysis rates were measured (Figure 1B). After hydrolysis, each tube was cooled by quenching in water for 10 min. The hydrolysate was filtered using 0.2 μm syringe filter prior to high pressure liquid chromatography (HPLC) analysis. Duplicate hydrolysis runs were made at each condition and the difference between the replicates was less than 5% for all data. Xylose and furfural yields were calculated based on

the composition of the xylo-oligosaccharide solution after addition of the acid.

HPLC analysis

Samples from sulfuric or oxalic acid-catalyzed hydrolysis were analyzed by Bio-Rad Aminex HPX-87H ion exchange column (300 mm \times 7.8 mm, Bio-Rad Laboratories Inc., Hercules, CA) connected to a Milton Roy mini pump (Milton Roy Co., Ivyland, PA), Waters™ 717 plus autosampler, and Waters™ 2414 refractive index detector (Waters Corp., Milford, MA). The mobile phase was 5 mM sulfuric acid in distilled, deionized water filtered through 0.2 μm . The mobile phase flow rate was 0.6 mL/min. The column temperature was maintained at 60°C by an Eppendorf CH-30

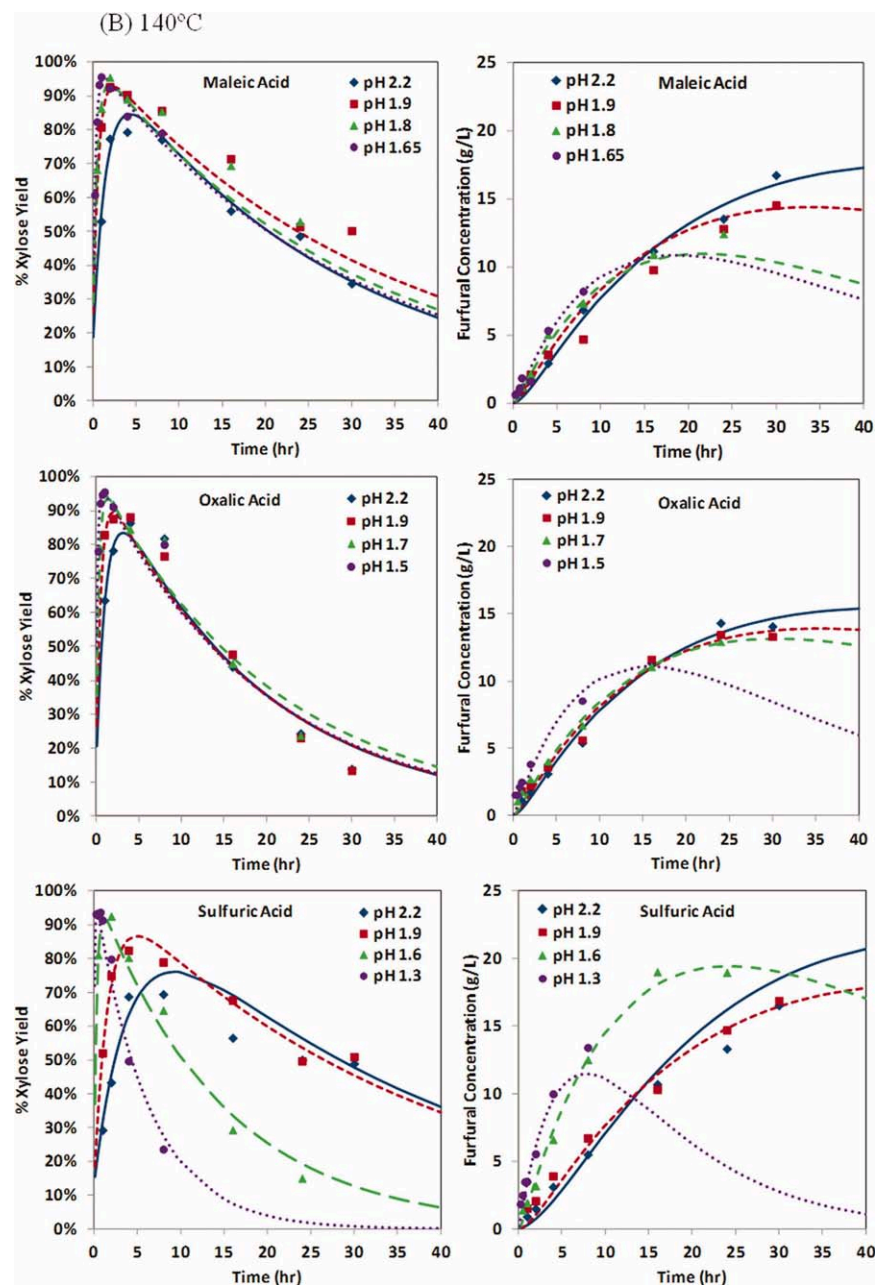


Figure 2.

Column Heater controlled by an Eppendorf TC-50 (Eppendorf, Westbury, NY). Calibration standards included glucose (0.5–4 g/L), xylose (0.5–4 g/L), acetone (0.25–2 g/L), hydroxymethylfurfural (HMF) (0.25–2 g/L), and furfural (0.25–2 g/L).

Maleic and oxalic acid-catalyzed reaction samples were analyzed by the same system with a mobile phase of 5% acetonitrile in 5 mM sulfuric acid filtered through 0.2 μm filter. The acetonitrile mobile phase was used for the maleic acid containing samples to separate xylose from fumaric acid, an isomer of maleic acid generated during the high-temperature hydrolysis step. Calibration standard solutions for maleic acid-catalyzed samples included malic acid (0.25–2 g/L) and fumaric acid (0.25–2 g/L) in addition to the aforementioned compounds. The data were stored and processed using EmpowerTM 2 Chromatography Data Software (Waters Corp., Milford, MA).

Parameter estimation

Kinetic rate equations as shown in the section entitled Reaction Model were used to fit the experimental data obtained at 140, 160, and 180°C and four different acid concentrations of each acid, giving the initial pH ranging from 1.3 to 2.2. The number of total experimental data points fitted for the model was 468 with duplicate hydrolysis runs. The rate constants (k) in the equations were determined by nonlinear least-squares fitting of the experimental data (xylose and furfural concentrations) using Microsoft Excel Solver pack as described by Kemmer and Keller.³⁸ The Arrhenius parameters, activation energy (E) and pre-exponential coefficients (k_0 , m), were determined by plotting natural log of rate constants (k) versus reciprocal of temperature ($1/T$) or natural log of hydronium ion concentrations, $[\text{H}^+]$. The resulting rate constants were then substituted into

Table 2. Determined Rate Constants for Acid Hydrolysis of Xylo-oligosaccharides at pH 1.9 (equivalent to $[H^+] = 13 \text{ mM}$)

	mM	Temp. (°C)	k_1 (1/h)	k_2 (1/h)	k_3 (1/h)	k_4 (1/h)	R^2 for [X]	R^2 for [F]	$\frac{k_1}{k_2+k_3}$
SA	26	140	0.63	0.02	0.01	0.02	0.92	0.97	23
		160	2.00	0.11	0.05	0.14	0.89	0.97	13
		180	6.46	0.46	0.36	0.24	0.94	0.98	8
MA	83	140	1.58	0.02	0.01	0.03	0.91	0.95	53
		160	5.58	0.09	0.05	0.05	0.96	0.99	39
		180	9.41	0.42	0.42	0.20	0.99	0.99	11
OA	44	140	1.72	0.02	0.03	0.01	0.95	0.97	32
		160	7.02	0.12	0.13	0.08	0.91	0.98	29
		180	18.99	0.47	0.75	0.14	0.90	0.96	16

*Selectivity for monosaccharide formation.

SA: sulfuric acid; MA: maleic acid; OA: oxalic acid.

Eqs. 5–7 and used to calculate the acid hydrolysis time course curves (solid lines) in Figure 2.

Results and Discussion

Xylose yields as a function of temperature and acid loading

Representative, experimental xylose yields and furfural concentration using dicarboxylic and sulfuric acids are summarized in Figure 2. The data points in Figure 2 are given as an example. Hydrolysis runs were carried out at a fixed pH of 1.9 at 140, 160, and 180°C for each acid. Figure 2B gives experimental hydrolysis time course at a fixed temperature of 140°C with variable acid loadings for each acid. Hydrolysis time course data were also obtained at fixed temperatures of 160 and 180°C while varying pH or at other fixed pH (1.3–2.2) with temperatures at 140, 160, and 180°C. These data consisted of over 250 conditions (time, temperature, and pH) with 468 duplicate measurements, in 36 graphs. Only one series (Figure 2) is shown here.

Xylose yields were inversely related to temperatures for all three acids. Hydrolysis at 140°C resulted in greater xylose yields with lower furfural formation. Higher acid loading (low pH) improved xylose yields while minimizing furfural formation.

Severity factors that gave maximum xylose yields occurred over a narrower range for carboxylic acids (maleic and oxalic acids) than for sulfuric acid. Optimal yields for sulfuric acid-catalyzed hydrolysis occurred at thermal severity factors of 2.5–3.9. For the diacids, maximum xylose yields occurred in a more narrow range of severity factors between 2.8 and 3.5. Hydrolysis of the xylo-oligosaccharide solution alone without addition of any acids (corresponds to acetic acid, pH 3.7) resulted in a maximum 36% yield ($\pm 9\%$) at a severity factor of 3.7 (data not shown).

Model fitting

Table 2 reports rate constants determined by the nonlinear least-squares fitting of the hydrolysis runs at a fixed pH of 1.9 with varying temperatures for each acid. Data for different pH values are not shown here. The R^2 -values of fitting between the calculations and experimental data were 0.9–0.99, indicating good fit of the model to the experimental results. The other rate constants were determined at different pH and temperatures, resulting in regression coefficient values (R^2) above 0.75, mostly in the range of 0.95–0.99. This demonstrated the suitability of the model for predicting the hydrolysis time courses. The lower R^2 values were due to the relatively low concentration of furfural concentration.

The experiments and theoretical predictions of xylose yields and furfural concentrations are presented in Figure 2. Lines represent the numerically determined responses (i.e., model) based on the kinetic constants obtained from the model fitting. The experimentally observed data and the predicted curves matched proving the capability of the model to give a quantitative interpretation of the experimental results.

The rate of xylo-oligomer hydrolysis to xylose was significantly higher than the rates of xylose degradation to furfural or to humins for all three acids. This indicated that the acid-catalyzed reaction favors the formation of xylose, rather than the degradation of xylose to furfural or other degradation products. As expected, all rate constants increased with temperature and acid concentrations. However, k_3 decreased with acid loadings for diacids. While k_3 for sulfuric acid increased with acid loadings, the k_3 for diacids decreased with increasing acid loadings (or hydronium ion concentrations). The dependence of the rate constants to acid concentrations was further examined by the Arrhenius plots and discussed in the following sections.

Arrhenius parameters

Representative Arrhenius plots showing the temperature and acid loading dependence of the rate constants are given in Figure 3. A linear relationship was found between $\ln(k)$ and $1/T$ or $\ln[H^+]$. Activation energy and pre-exponential factors were determined for each temperature and pH condition. The obtained activation energy varied within a narrow range for the acid loadings tested. Therefore, an averaged activation energy was taken to further determine the pre-exponential factors (Tables 3 and 4). The Arrhenius equation provided an excellent interpretation of the results, judging by the R^2 values.

Temperature Dependence of Rate Constants. Temperature dependence of the hydrolysis kinetics is represented in Figure 3A. The slope in Figure 3A gives activation energy for each reaction step. The Student's t test showed no significant difference in the activation energy for hydrolysis between the acids ($P > 0.05$) (Table 3). Consistent with the highest measured rate constants for k_1 , the activation energy for the hydrolysis of xylo-oligomers to xylose was the lowest. The hydrolysis step is less affected by temperature change than degradation where the energy of activation is larger. The relatively higher activation energy for degradation reactions indicates that the degradation process is more temperature sensitive than the hydrolysis reaction. Accordingly, increasing reaction temperature imposes negative

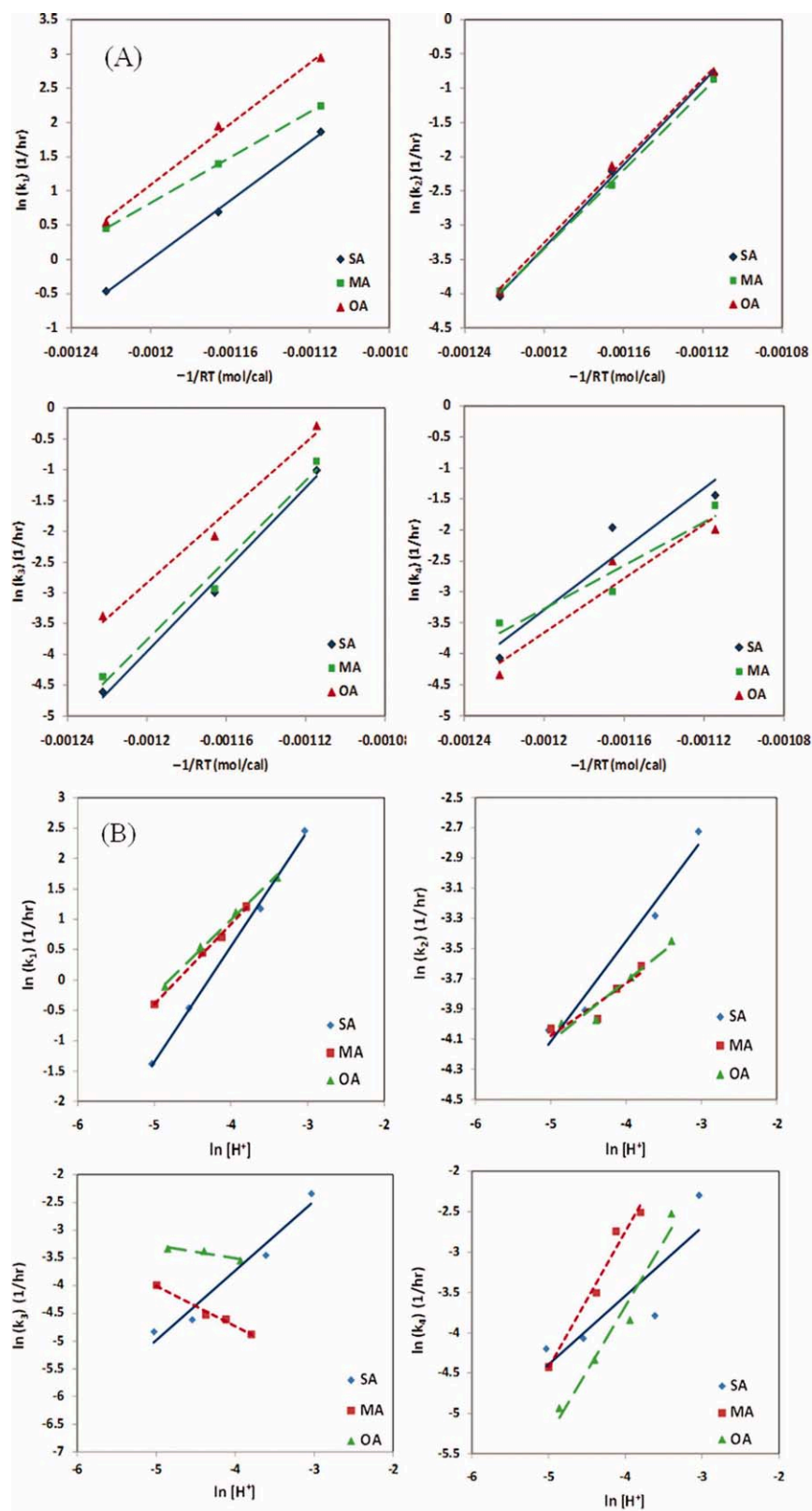


Figure 3. Representative Arrhenius plots showing (A) the temperature dependence of the kinetic rate constants, k_{1-4} for estimation of activation energy, E at pH 1.9; (B) the acid dependence of the kinetic rate constants, k_{1-4} for estimation of pre-exponential factor parameters, k_0 and m at 140°C .

SA: sulfuric acid; MA: maleic acid; OA: oxalic acid. [Color figure can be viewed in the online issue, which is available at wileyonlinelibrary.com.]

Table 3. Arrhenius Activation Energy (E) for Acid Hydrolysis of Xylo-oligosaccharides

Activation Energy (kJ/mol)	SA	MA	OA
E_1	89.4 ± 11.3 ($R^2 = 0.99$)	83.5 ± 9.6 ($R^2 = 0.98$)	88.4 ± 11.5 ($R^2 = 0.98$)
E_2	115.8 ± 7.5 ($R^2 = 0.99$)	119.8 ± 3.1 ($R^2 = 0.98$)	122.7 ± 6.1 ($R^2 = 0.99$)
E_3	130.6 ± 15.0 ($R^2 = 0.97$)	128.9 ± 10.3 ($R^2 = 0.99$)	107.7 ± 16.4 ($R^2 = 0.99$)
E_4	103.5 ± 2.9 ($R^2 = 0.87$)	87.8 ± 27.8 ($R^2 = 0.97$)	114.5 ± 11.3 ($R^2 = 0.93$)

Errors represent 95% CI.

impacts on maximizing xylose yields, as an increase of temperature is more influential on monosaccharide degradation reactions than on hydrolysis of sugar oligomers.

The activation energy of xylo-oligomers hydrolysis ($E_1 = 84$ kJ/mol) for maleic acid in this study was comparable to the previously reported 83.3 kJ/mol.¹⁰ Our value of activation energy for the furfural formation ($E_2 = 120$ kJ/mol) was lower than the 143.5 kJ/mol reported by Lu and Mosier.¹⁰ Nonetheless, all of the results were consistent. Lower temperature favors xylose yields from maleic acid due to lower energy barrier (activation energy) for hydrolysis than for degradation and gave maximal yields. Values of activation energy for oxalic acid also showed a lower sensitivity to temperature for hydrolysis ($E_1 = 88$ kJ/mol) than aldehydes formation ($E_2 = 123$ kJ/mol). Another study by Kim et al.¹⁶ showed higher xylose recovery at lower temperature when oxalic acid was used at 160–180°C. The lower E_1 values were also reported by Garrote et al.⁸ for autohydrolysis of soluble xylo-oligomers derived from eucalyptus wood. The activation energy of hydrolysis of xylo-oligosaccharide hydrolysis was 102–108 kJ/mol, which was slightly lower than the activation energy of xylose degradation at 109–144 kJ/mol.⁸

Activation energy for sulfuric acid in our study gave somewhat contradictory results to previous work that reported higher activation energy for xylan hydrolysis than for xylose degradation.^{2,39} Thus, previous work concluded that higher temperature is beneficial to maximize xylose yield when inorganic acids such as sulfuric or hydrochloric acids are used. The difference is probably due to the choice of substrate. These previous studies used solid hemicellulose (xylan) embedded in lignocellulose substrate, while we used soluble xylan. Hemicellulose embedded in a complex matrix of lignocellulose components is more difficult to hydrolyze due to mass-transfer limitation of acid and heterogeneity of hemicellulose compositions, thus resulting in higher apparent activation energy (i.e., higher energy barrier) than soluble xylo-oligomers.

pH Dependence of Rate Constants. The dependence of rate kinetics on hydronium concentration is depicted in Figure 3B and Table 4. The pre-exponential factor, K , correlates the rate constants with $[H^+]$, through the empirical coefficient, m . Hydrolysis rate constants (k_1) increase with increasing hydronium ion (H^+) concentration for both sulfuric acid and diacids. The rate of furfural formation from

xylose also increases (k_2 versus $[H^+]$) as a function of diacid concentration. Maleic and oxalic acids are different from sulfuric acid in three ways; (1) The steepness (m) of increasing rates of hydrolysis (k_1) and furfural formation (k_2) with $[H^+]$ is lower than for sulfuric acid. This indicates that selectivity to xylose formation for diacids increases with acid dose and the beneficial effect becomes more pronounced than for sulfuric acid as pH decreases; (2) the formation of humic substances through xylose degradation (k_3) decreases with $[H^+]$ or is lower at high acid concentration for diacids. Sulfuric acid shows the opposite; (3) the rate of humic substances formation (k_4) from furfural at a lower acid (H^+) concentration is higher for sulfuric acid.

The m values determined for hydrolysis ($m = 1.23$ for k_1) and furfural formation ($m = 0.25$ for k_2) steps in the maleic acid-catalyzed hydrolysis runs were comparable to those measured in Lu and Mosier¹⁰ who reported 1.6 and 0.42 for the equivalent steps using corn stover hemicellulose as substrate.

The negative m values for k_3 in dicarboxylic acid-catalyzed hydrolysis mean that adding more acids prevents xylose degradation to humic substances. The opposite effect occurs for sulfuric acid. The observations are not explained by traditional acid-catalyzed hydrolysis kinetics for which sugar degradation increases with hydronium ion concentrations. Unlike strong mineral acids that follow specific acid catalysis mechanism in which the rate of xylose degradation solely depends on the proton concentrations, maleic acid-mediated catalyst involves a protective action of maleate ion on xylose dehydration, which is not explained by either specific acid or general acid mechanism.^{10,22} The maleate ion may form a strong internal hydrogen bond with xylose transition-state intermediate, inhibiting the intermediate from further degrading.²² Mosier et al.¹² and Kootstra et al.^{13,14,20} reported that maleic acid below a certain concentration of 200 mM showed comparable or lower rates of sugar degradation than pure water. Sulfuric acid gave a strong sugar degradation effect at the same concentration. Kootstra et al.²⁰ also tested fumaric acid, another weak dicarboxylic acid, which displayed a stabilizing effect on arabinose, reducing its degradation. Fumaric acid is also an isomer of maleic acid formed during heat treatment of maleic acid.^{40,41} Oxalic acid is assumed to follow the same catalysis mechanisms as maleic acid, given the proximity to maleic acid in terms of structural and acidic characteristics.

Table 4. Arrhenius Pre-Exponential Factor Parameters, k_0 and m for Acid Hydrolysis of Xylo-oligosaccharides

Pre-exponential Factor, K	SA			MA			OA		
	m	k_0 (1/h)	R^2	m	k_0 (1/h)	R^2	m	k_0 (1/h)	R^2
K_1	1.74	4.3×10^{14}	0.98	1.23	0.15×10^{14}	0.93	0.93	0.29×10^{14}	0.99
K_2	0.72	3.2×10^{14}	0.83	0.25	1.1×10^{14}	0.71	0.42	4.8×10^{14}	0.84
K_3	1.12	740×10^{14}	0.97	−0.56	0.3×10^{14}	0.80	−0.38	0.004×10^{14}	0.81
K_4	0.88	0.1×10^{14}	0.86	2.35	0.8×10^{14}	0.91	1.71	150×10^{14}	0.92

Errors represent 95% CI.

SA: sulfuric acid; MA: maleic acid; OA: oxalic acid.

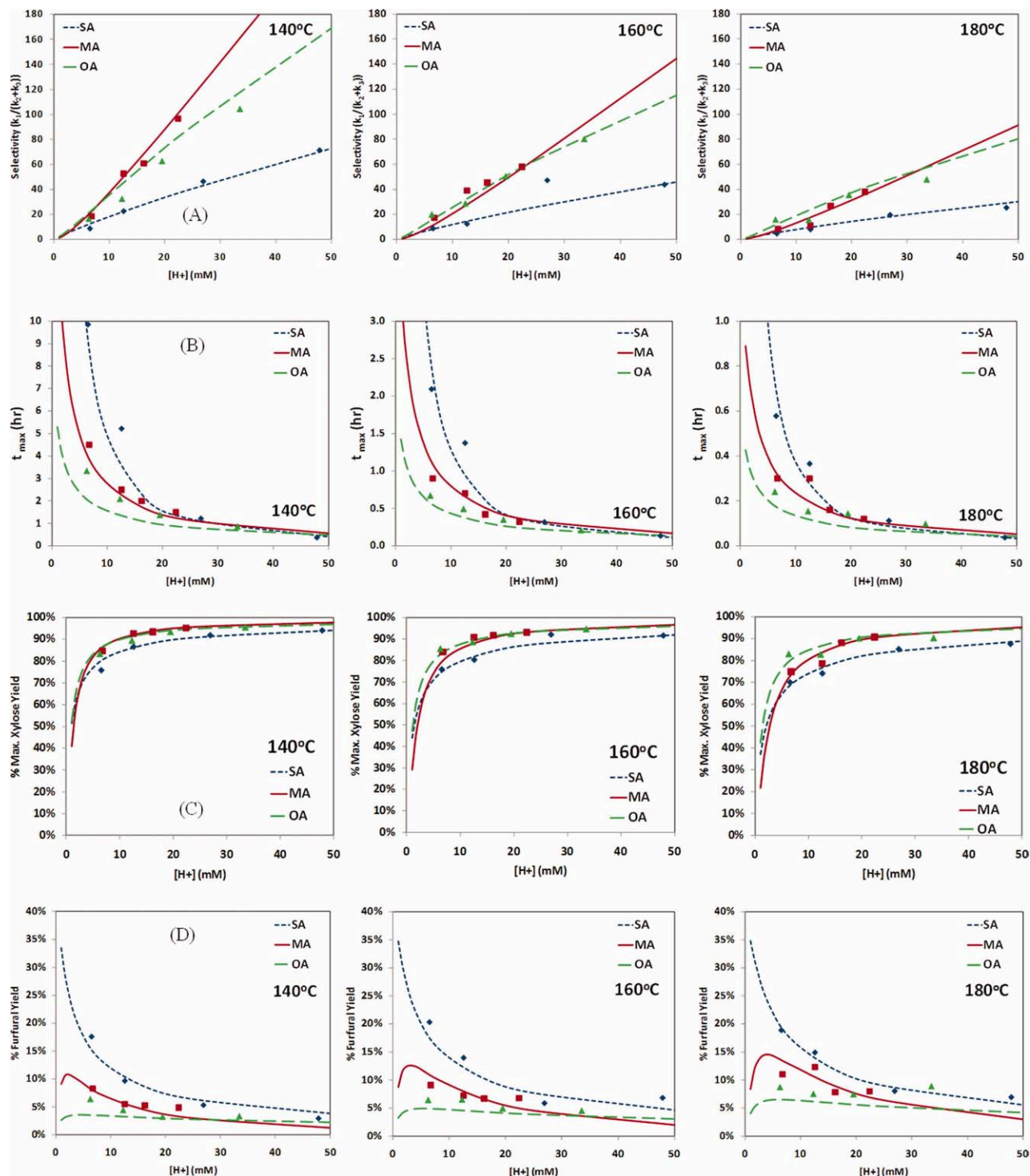


Figure 4. Calculated (A) selectivity factors; (B) t_{\max} ; (C) maximum xylose; and (D) furfural yields at t_{\max} at different hydrogen ion concentrations.

Symbols represent calculated values based on the experimentally determined rate constants at each specific hydrolysis condition. Lines represent calculated values based on the averaged rate constant parameters in Tables 3 and 4. SA: sulfuric acid; MA: maleic acid; OA: oxalic acid. [Color figure can be viewed in the online issue, which is available at wileyonlinelibrary.com.]

The determined rate constants and analysis of Arrhenius plots suggest that a low-temperature and low pH (high acid dose) are desirable for both sulfuric and dicarboxylic acids. The beneficial effect is pronounced for diacids, consistent with their previously reported protective effect.¹⁰

Model validation

The kinetic constants and parameters as determined for each hydrolysis condition based on the model successfully responded to the experimental data for all three acids (Figure 2, Table 2). The averaged activation energy and pre-exponential parameters summarized in Tables 3 and 4 were

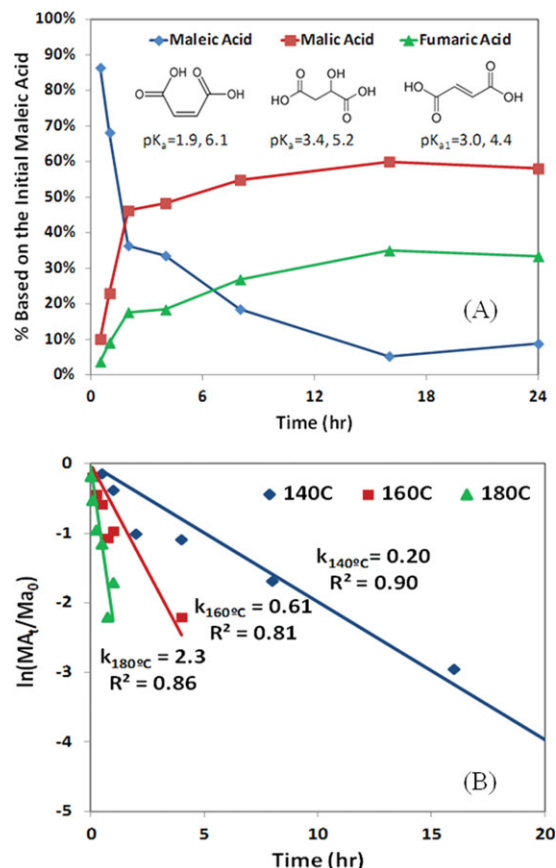


Figure 5. (A) Thermal isomerization and hydration of maleic acid to fumaric and malic acids as a function of hydrolysis time at 140°C; (B) a plot of $\ln(MA_t/MA_0)$ as a function of hydrolysis time at 140, 160, and 180°C.

Initial maleic acid concentration: 108 mM (pH 1.8). Data represent average of duplicate measurements. [Color figure can be viewed in the online issue, which is available at [wileyonlinelibrary.com](http://www.interscience.wiley.com).]

further used for the validation of the model. Figure 4 provides calculated selectivity factors, t_{\max} , and corresponding maximum xylose yields and furfural formation at t_{\max} as a function of hydronium concentration. Symbols in Figure 4 were calculated from the rate constants, which were individually determined by the model fitting of the experimental data at each specific hydrolysis condition. For example, the symbols at $[H^+] = 13$ mM were calculated from the rate constants given in Table 2. Lines represent the calculations from the generalized kinetic rate parameters summarized in Tables 3 and 4. Good agreement was found between the predictions by the condition-specific rate constants and those used in the generalized rate equations.

Selectivity Factor. Both measured and calculated selectivity factors followed the order of maleic acid \geq oxalic acid $>$ sulfuric acid at equivalent H^+ concentrations (Table 2, Figure 4A). The selectivity factor increased with acidity of the reaction solution and decreased with temperature. The results accord with the interpretation of Arrhenius coefficients that concluded earlier that a combination of low-temperature and high acid loading is desirable for maximizing xylose yields. As the pH decreases, the difference in hydrolysis rates (k_1) becomes smaller, while sugar degradation than diac-

ids at the same conditions (Figure 3B and Tables 3 and 4), due to the protective effects of maleic and oxalic acids.

t_{\max} . The time at which maximal conversion of xylo-oligosaccharide to xylose occurs is a function of k_1 , k_2 , and k_3 (Eq. 8). These constants are in turn a function of temperature, type of acid, and concentration of acid. Raising hydrolysis temperature and increasing acid loading significantly reduces t_{\max} (see Figure 4B). For example, at pH 1.9, which is equivalent to $[H^+] = 13$ mM, optimum hydrolysis occurs at 140°C/2.5 h for maleic acid. Increasing temperature from 140 to 180°C reduces the reaction time by approximately 10 times at equivalent pH. Lowering pH by 0.2–0.3, which is equivalent to adding 2–4 times more acids by weight, reduces hydrolysis time by a factor of 2–3.

The t_{\max} for sulfuric acid was significantly higher than for dicarboxylic acids at the same pH. The difference appeared to diminish as the acidity of solution increases. At the highest pH (pH > 2.0), the hydrolysis rate constant, k_1 , for sulfuric acid was significantly lower than for maleic or oxalic acid, thus requiring a longer reaction time to reach the optimal xylose yield. At pH lower than 2.0, the difference in k_1 is reduced between the acids, while sugar degradation rates (k_2 and k_3) for sulfuric acid became much greater than those of dicarboxylic acid.

Xylose Yields, Furfural Formation at t_{\max} . Maleic and oxalic acids maximize xylose yields and minimize furfural formation at any given pH (Figures 4C, D), due to their distinctive effect on preventing xylose degradation. In comparison, sulfuric acid generated two- to three-fold more furfural than dicarboxylic acids, while xylose yields were lower by 5–10% at its optimal condition. At 140°C, the maximum xylose yield was 85–90% at 50–83 mM maleic acid or 33–44 mM oxalic acid (pH 1.9–2.2). Sulfuric acid gave a similar extent of xylose yield (Figure 4C) at a lower pH range (pH < 1.6). Hence, sulfuric acid may demand more corrosion resistant materials for design of reactors and equipment that would achieve high xylose yields ($>90\%$).

Hydrolysis at 120°C. Analysis of the experimentally and numerically determined rate constants and the Arrhenius plots demonstrated that low-temperatures and high acid loadings are advantageous for increasing maximum xylose yields. To validate the model for hydrolysis at a low-temperature, hydrolysis was carried out at 120°C using 83 mM maleic acid, and the results were compared to those predicted by the model. The 83 mM sulfuric acid (pH 1.9) at 120°C for 16 h ($\log R_0 = 3.6$) resulted in $96.7 \pm 2.8\%$ xylose yield with 2.5 ± 0.2 g/L furfural. The model estimated 92.0% xylose yield and 2.7 g/L furfural. Thus, near-quantitative xylose yields were achieved using maleic acid at 120°C and the model predicted the yields and furfural formation well with only slight deviations. Increase of acid will further improve the xylose yield but only a minimal extent ($<5\%$). Thus, adding more acid is not beneficial as increased catalyst (acid) cost and drop of pH would negate the yield benefit.

Thermal stability of dicarboxylic acids

The pH of the hydrolysis solution at the end of the hydrolysis increased by 0.1–0.4 pH units for the maleic and oxalic acid-catalyzed solutions. This is likely due to thermal conversion of dicarboxylic acids to weaker acids and/or release of acetic acid ($pK_a = 4.8$) from the hydrolyzed xylo-oligosaccharides. There was no pH change for the sulfuric acid-catalyzed solutions.

At temperatures above 130°C, maleic acid isomerizes to fumaric acid ($pK_a = 3.0$ and 4.4) or hydrates into malic acid ($pK_a = 3.4$ and 5.2).^{14,40,41} Fumaric acid is suggested as an alternative to sulfuric acid due to reduced formation of fermentation inhibitors (furfural) compared to sulfuric acid.¹⁴ Given the possibility of thermal degradation, we measured malic and fumaric acid formation in the xylo-oligosaccharide solution. The maleic acid that remained was calculated by subtracting the measured malic and fumaric acids from the initial maleic acid. At 108 mM initial maleic acid (pH 1.8) and 140°C, isomerization and hydration of maleic acid were significant with 90% of the maleic acid being converted to fumaric and malic acids in 15 h at a 6:4 malic to fumaric acid ratio (Figure 5A). The thermal disappearance of maleic acid followed a logarithmic decline, which was fitted by a first-order, thermal deactivation of catalyst⁴²:

$$MA_t = MA_0 e^{-kt} \quad (15)$$

in which MA_t = maleic acid concentration at time t ; MA_0 = initial maleic acid concentration; k = rate constant; and t = time (h). A plot of natural log of MA_t/MA_0 versus time gave the maleic acid's degradation rate constant, k as a slope (Figure 5B). As shown in Figure 5B, the thermal conversion of maleic acid to fumaric and malic acid followed the first-order decline with respect to time. The determined k was a function of temperature, giving a higher value at high-temperature than at low-temperature. Maleic acid's isomerization and hydration was 10 times faster at 180°C than at 140°C.

Oxalic acid is known to decompose to formic ($pK_a = 3.8$) and carbonic acids ($pK_a = 3.6$, 10.3) in aqueous solutions at temperatures ranging from 180 to 230°C.⁴³ In this study, we could not trace oxalic acid and its degradation in hydrolysates due to analytical limitations, as the sugar oligomers coeluted with oxalic acid. Thermal treatment of 10 g/L oxalic acid in DI water at 200°C for 10 min indicated nearly all oxalic acid was decomposed.

Cost considerations

Sulfuric acid is the least expensive acid among the acids tested in this study. However, the sulfuric acid cost advantage is partially negated by the fact that it requires a lower pH to achieve an equivalent level of xylose yields as dicarboxylic acid. Sulfuric acid has a higher neutralization cost and may be accompanied by high capital cost of the equipment and reactor materials of construction for dealing with its corrosive nature. It also generates more fermentation inhibitors than dicarboxylic acids and this adds cost to the overall process.

Limitations of maleic acid would mainly reside in the high cost of the acid itself. Maleic acid and oxalic acid are approximately 7–10 times and 2–3 times more costly than sulfuric acid, respectively.^{9,14} Its high acid cost, however, can be partly compensated by higher return on xylose yield and reduced sugar loss to degradation (less amounts of fermentation inhibitors) compared to sulfuric acid. Moreover, the dicarboxylic acids are less corrosive than sulfuric acid.

After the hydrolysis step is completed, the acid must be neutralized so that the solution pH may be adjusted to 5.5–6.0 prior to fermentation. Sulfuric acid-catalyzed hydrolysates require that gypsum or NH_4OH be added to neutralize. In a self-limiting process, maleic acid thermally degrades to malic and fumaric, which requires less base for neutralization.

Conclusions

Analysis of empirical data and model parameters explicitly indicated that: (1) hydrolysis of soluble sugar oligomers in washate stream of steam exploded mixed hardwood follows first-order hydrolysis kinetics; (2) a combination of low-temperature and high acid loading leads to increased xylose yields and minimal sugar loss to degradation; (3) dicarboxylic acids outperform sulfuric acid by preventing xylose degradation; (4) xylose degradation rate by dicarboxylic acids is inversely dependent on pH; (5) sulfuric acid requires a lower pH than dicarboxylic acid to give an equivalent level of optimal xylose yield. A monophasic model based on Saeman's pseudohomogeneous irreversible first-order reaction kinetics and specific acid catalysis successfully modeled hydrolysis of wood-derived xylo-oligosaccharide by dicarboxylic acids.

Acknowledgments

The material in this work was supported by Mascoma Corporation and the US Department of Energy (contract #DE-F-08G018103). We thank Todd Lloyd, David Hogsett, and Yulin Lu for providing xylo-oligomer containing sugar stream used in this work. The authors also thank Nathan S. Mosier and Elizabeth Casey of Purdue University and David Hogsett, and William Kenealy of Mascoma for their internal review of this paper and helpful suggestions. Michael R. Ladisch is CTO at Mascoma Corporation.

Literature Cited

- Girio FM, Fonseca C, Carvalho F, Duarte LC, Marques S, Bogel Lukasik R. Hemicelluloses for fuel ethanol: a review. *Bioresour Technol.* 2010;101:4775–4800.
- Ladisch MR. *Hydrolysis*. In: Kitani O, Hall CW, editors. *Biomass Handbook*. New York: Gordon & Breach Science Publishers, 1989:434–451.
- Wyman CE, Decker SR, Himmel ME, Brady JW, Skopec CE, Viikari L. *Hydrolysis of cellulose and hemicellulose*. In: Dumitriu S, editor. *Polysaccharides: Structural Diversity and Functional Versatility*. New York: Marcel Dekker, Inc., 2005:995–1033.
- Mosier NS, Wyman C, Dale B, Elander R, Lee YY, Holtzapple M, Ladisch MR. Features of promising technologies for pretreatment of lignocellulosic biomass. *Bioresour Technol.* 2005;96:673–686.
- Kim YM, Hendrickson R, Mosier NS, Ladisch MR. *Liquid hot water pretreatment of cellulosic biomass*. In: Mielenz JR, editor. *Methods in Molecular Biology: Biofuels*. Totowa, NJ: The Humana Press, Vol. 581, 2009:93–102.
- Kim YM, Mosier NS, Ladisch MR. Enzymatic digestion of liquid hot water pretreated hybrid poplar. *Biotechnol Prog.* 2009;25:340–348.
- Kim YM, Hendrickson R, Mosier NS, Ladisch MR. Plug-flow reactor for continuous hydrolysis of glucans and xylans from pretreated corn fiber. *Energy Fuels.* 2005;19:2189–2200.
- Garrote G, Domínguez H, Parajó JC. Generation of xylose solutions from *Eucalyptus globulus* wood by autohydrolysis-posthydrolysis processes: posthydrolysis kinetics. *Bioresour Technol.* 2001;79:155–164.
- Lu Y, Mosier NS. Biomimetic catalysis for hemicellulose hydrolysis in corn stover. *Biotechnol Prog.* 2007;23:116–123.
- Lu Y, Mosier NS. Kinetic modeling analysis of maleic acid-catalyzed hemicellulose hydrolysis in corn stover. *Biotechnol Bioeng.* 2008;101:1170–1181.
- Mosier NS, Sarikaya A, Ladisch CM, Ladisch MR. Characterization of dicarboxylic acids for cellulose hydrolysis. *Biotechnol Prog.* 2001;17:474–480.
- Mosier NS, Ladisch CM, Ladisch MR. Characterization of acid catalytic domains for cellulose hydrolysis and glucose degradation. *Biotechnol Bioeng.* 2002;79:610–618.
- Kootstra AM, Beftink HH, Scott EL, Sanders JPM. Comparison of dilute mineral and organic acid pretreatment for enzymatic hydrolysis of wheat straw. *Biochem Eng J.* 2009;46:126–131.
- Kootstra AM, Beftink HH, Scott EL, Sanders JPM. Optimization of the dilute maleic acid pretreatment of wheat straw. *Biotechnol Biofuel.* 2009;2:Paper 31.

15. Shimada M, Ma DB, Akamatsu Y, Hattori T. A proposed role of oxalic acid in wood decay systems of wood-rotting Basidiomycetes. *FEMS Microbiol Rev.* 1994;13:285–296.
16. Kim HY, Lee JW, Jeffries TW, Choi IG. Response surface optimization of oxalic acid pretreatment of yellow poplar (*Liriodendron tulipifera*) for production of glucose and xylose monosaccharides. *Bioresour Technol.* 2011;102:1440–1446.
17. Lee JW, Jeffries TW. Efficiencies of acid catalysts in the hydrolysis of lignocellulosic biomass over a range of combined severity factors. *Bioresour Technol.* 2011;102:5884–5890.
18. Lee JW, Rodrigues RCLB, Jeffries TW. Simultaneous saccharification and ethanol fermentation of oxalic acid pretreated corncob assessed with response surface methodology. *Bioresour Technol.* 2009;100:6307–6311.
19. Lee JW, Rodrigues RCLB, Kim HY, Choi IG, Jeffries TW. The roles of xylan and lignin in oxalic acid pretreated corncob during separate enzymatic hydrolysis and ethanol fermentation. *Bioresour Technol.* 2010;101:4379–4385.
20. Kootstra AM, Mosier NS, Scott EL, Beftink HH, Sanders JPM. Differential effects of mineral and organic acids on the kinetics of arabinose degradation under lignocellulose pretreatment conditions. *Biochem Eng J.* 2009;43:92–97.
21. Rye CS, Withers SG. Glycosidase mechanisms. *Curr Opin Chem Biol.* 2000;4:573–580.
22. Lu Y. Kinetic and mechanistic studies of a biomimetic catalyst for hemicellulosic biomass hydrolysis. Ph.D. Thesis, Purdue University, 2008.
23. Saeman JF. Kinetics of wood saccharification-hydrolysis of cellulose and decomposition of sugars in dilute acid at high temperature. *Ind Eng Chem.* 1945;37:43–52.
24. Kobayashi T, Sakai Y. Hydrolysis rate of pentosan of hardwood in dilute sulfuric acid. *Bull Agric Chem Soc Jpn.* 1956;20:1–7.
25. Maloney MT, Chapman TW, Baker AJ. Dilute acid hydrolysis of paper birch: kinetics studies of xylan and acetyl group hydrolysis. *Biotechnol Bioeng.* 1985;27:355–361.
26. Mittal A, Chatterjee SG, Scott GM, Amidon TE. Modeling xylan solubilization during autohydrolysis of sugar maple and aspen wood chips: reaction kinetics and mass transfer. *Chem Eng Sci.* 2009;64:3031–3041.
27. Carvalheiro F, Garrote G, Parajó JC, Pereira H, Gírio FM. Kinetic modeling of brewery's spent grain autohydrolysis. *Biotechnol Prog.* 2005;21:233–43.
28. Brennan MA, Wyman CE. Initial evaluation of simple mass transfer models to describe hemicellulose hydrolysis in corn stover. *Appl Biochem Biotechnol.* 2004;115:965–976.
29. Root DF. Kinetics of the acid catalyzed conversion of xylose to furfural. Ph.D. thesis, University of Wisconsin, 1956.
30. Harris JF, Baker AJ, Conner AH, Jeffries TW, Minor JL, Peterson RC, Scott RW, Springer EL, Wegner TH, Zerbe JL. Two-stage, dilute sulfuric acid hydrolysis of wood: investigation of fundamentals. *USDA Forest Service Report FPL-45*, 1985.
31. Weingarten R, Cho J, Conner WC, Huber GW. Kinetics of furfural production by dehydration of xylose in a biphasic reactor with microwave heating. *Green Chem.* 2010;12:1423–1429.
32. Antal MJ, Leesomboon T, Mok W. Mechanism of formation of 2-furaldehyde from D-xylose. *Carbohydr Res.* 1991;217:71–85.
33. Marshall WL, Jones EV. Second dissociation constant of sulfuric acid from 25 to 350° evaluated from solubilities of calcium sulfate in sulfuric acid solutions. *J Phys Chem.* 1966;70:4028–4040.
34. Thakur P, Mathur JN, Moore RC, Choppin GR. Thermodynamics and dissociation constants of carboxylic acids. *Inorg Chim.* 2007;360:3671–3680.
35. Sue K, Ouchi F, Minami K, Arai K. Determination of carboxylic acid dissociation constants to 350°C at 23 MPa by potentiometric pH measurements. *J Chem Eng Data.* 2004;49:1359–1363.
36. Overend RP, Chornet E. Fractionation of lignocellulosics by steam-aqueous pretreatment. *Phil Trans R Soc London Ser A.* 1987;321:523–536.
37. Sluiter A, Hames B, Ruiz R, Scarlata C, Sluiter J, Templeton D. Determination of sugars, byproducts, and degradation products in liquid fraction process samples. Biomass analysis technology team laboratory analytical procedures (LAP 014). NREL Biomass Program, 2005.
38. Kemmer G, Keller S. Nonlinear least-squares data fitting in excel spreadsheets. *Nat Protoc.* 2010;5:267–280.
39. Bhandari N, Macdonald DG, Bakhshi NN. Kinetic studies of corn stover saccharification using sulfuric acid. *Biotechnol Bioeng.* 1984;26:320–327.
40. Weiss JM, Downs CR. Preliminary study on the formation of malic acid. *J Am Chem Soc* 1922;44:1118–1125.
41. Felthouse TR, Burnett JC, Horrell B, Mummey MJ, Kuo YJ. *Maleic anhydride, maleic acid, and fumaric acid*. In: Humphreys L, Aitieri L, editors. *Encyclopedia of Chemical Technology*. New York: John Wiley and Sons, 1995:893–928.
42. Kim Y, Hendrickson R, Mosier NS, Ladisch MR. Plug-flow reactor for continuous hydrolysis of glucans and xylans from pretreated corn fiber. *Energy Fuels.* 2005;19:2189–2200.
43. Crossey LJ. Thermal degradation of aqueous oxalate species. *Geochem Cosmochim Acta.* 1991;55:1515–1527.

Manuscript received Dec. 22, 2011, and revision received Mar. 12, 2012.